CASL-U-2014-0143-000

Power uprates
and plant life extension

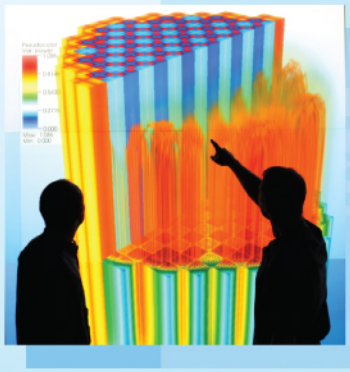

Engineering design
and analysis

Science-enabling
high performance
computing

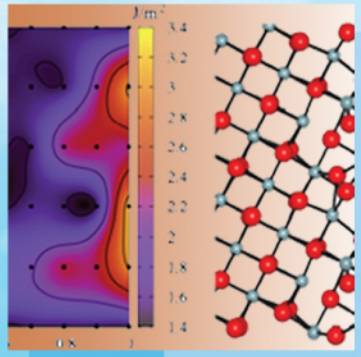

Fundamental science

Plant operational data

Consortium for Advanced Simulation of LWRs

L3:MPO.CRUD.P8.02

Two-Phase Fluid Flow Modeling in CRUD using MAMBA-BDM

Miaomiao Jina and Michael Short
Massachusetts Institute of Technology

February 17, 2014

U.S. DEPARTMENT OF ENERGY | Nuclear Energy

Two-Phase Fluid Flow Modeling in CRUD using MAMBA-BDM

Miaomiao Jin[a], Prof. Michael Short[a,*]

[a]*Massachusetts Institute of Technology, 77 Massachusetts Ave., Cambridge, MA 02139*

Abstract

CRUD is a CASL challenge problem with a significant component in the Materials Performance and Optimization (MPO) focus area. CRUD buildup can give rise to axial offset anomaly (AOA), a spatial flux tilting due to local boron concentration, and to CRUD-induced localized corrosion (CILC), accelerated chemical attack coupled to temperature. The second of these problems is being treated by the MAMBA-BDM mesoscale CRUD multiphysics model. However, recent reports and publications revealed that two-phase heat transfer within the CRUD cannot be neglected, and that assumptions made by most previous CRUD models of wick boiling and fluid superheating at high pressures cannot be true.

We report on changes to the MAMBA-BDM model, incorporating separate, but coupled, regions of liquid and vapor flow within the CRUD. The treatment of two separate phases, as well as eliminating the wick boiling assumption at the CRUD-boiling chimney interface, has led to predictably higher peak cladding temperatures for a given simulation. Implications for CILC are significant: according to recent MPO modeling efforts, peak clad temperature changes like those observed in this report can make the difference between asymptotic and breakaway Zircaloy oxidation. Ongoing efforts to re-run full-core simulations with these new models, as well as a full-core CILC estimation, are discussed.

MPO L3 Milestone (Due Feb. 15, 2014): Create dimension-agnostic model in MAMBA-BDM for vapour dryout in the CRUD, modeled as 2-phase Darcy flow

*Corresponding author
Email addresses: mmjin@mit.edu (Miaomiao Jin), hereiam@mit.edu (Prof. Michael Short)

Contents

1 Introduction **5**

2 Background **5**

2.1 Previous CRUD Modeling Efforts 6

2.2 Requirements for an Accurate Two-Phase CRUD Model 9

3 Changes to MAMBA-BDM's Framework **10**

3.1 Overall Description 10

3.2 Correlations and Boundary Conditions Changed in MAMBA-BDM 11

4 New Results **11**

4.1 Two-Phase Modeling Results 11

4.2 Comparison of One-Phase and Two-Phase Results 12

5 Discussion **12**

6 Future Work **14**

6.1 Areas for Improvement 14

7 Acknowledgements **15**

References **15**

Acronyms, Definitions and Symbols Used

Term	Definition
CASL	Consortium for Advanced Simulation of Light-water reactors
CCM	CRUD Chemistry Model
CILC	CRUD-Induced Localized Corrosion (accelerated clad corrosion due to an extreme environment inside CRUD)
CIPS	CRUD-Induced Power Shift (same as AOA)
CRUD	Chalk River Unidentified Deposits (a generic term for unwanted deposits on reactor surfaces, usually the fuel)
EPRI	Electric Power Research Institute
MAMBA	MPO Advanced Model for Boron Analysis
MPO	Materials Performance and Optimization
PWR	Pressurized Water Reactor
TKE	Turbulent Kinetic Energy

Symbol	Definition	Units
h_{fg}	Heat of vaporization	$\frac{\mathrm{W}}{\mathrm{m}^2\mathrm{K}}$
i,j	Node indices (i for x, j for y)	—
k	Thermal conductivity	$\frac{\mathrm{W}}{\mathrm{mK}}$
$\dot{\mathrm{m}}$	Mass flow rate	$\frac{\mathrm{kg}}{\mathrm{s}}$
$\overrightarrow{n}$	Normal direction	—
t	Time	s
v	Fluid velocity	$\frac{\mathrm{m}}{\mathrm{s}}$
A_c	Cross sectional area for flow	m^2
C	Concentration	mole frac.
D_h	Hydraulic diameter	m
P	Pressure	Pa
$\dot{Q}$	Heat Flux	$\frac{\mathrm{W}}{\mathrm{m}^2}$
T	Temperature	K
ε	Porosity	—
η	Fluid shear viscosity	$\mathrm{Pa} \cdot \mathrm{s}$
κ	Darcy flow permeability	m^2
λ	Pore size (diameter or equivalent)	m
μ	Mobility of a particle in a fluid	$\mathrm{Pa} \cdot \mathrm{m} \cdot \mathrm{s}$
ρ	Density	$\frac{\mathrm{kg}}{\mathrm{m}^3}$
σ	Surface tension	$\frac{\mathrm{N}}{\mathrm{m}}$
τ_{avg}	Average tortuosity for flowpaths and diffusion	—
θ_c	Contact angle	degrees
Γ, γ	Boundary (partial or full) around a space Ω	—

1. Introduction

After three years of CRUD modeling within CASL, from atomistic scale simulations, to micro/mesoscale calculations, to pin-level and full-core analyses, it has become clear that the existing models of fluid flow within CRUD do not account for the effects observed. In particular, longstanding assumptions of wick boiling at the boundary between porous CRUD and the boiling chimneys found throughout must assume large amounts of liquid superheating (10-15K) at high pressures (15.5MPa) to reach closure. These assumptions have been shown to be unphysical in recent conference talks [1] and literature publications [2] by members of CASL. These results, coupled with recent predictions of resultant Zircaloy breakaway oxidation underneath CRUD [3], known as CRUD-induced localized corrosion (CILC), can help determine whether the tracking of liquid and vapor regions in the CRUD can explain the expected higher temperature at the surface of the cladding, and the resultant accelerated corrosion rate underneath.

In order to reconcile these incorrect assumptions, the flow and creation of two-phase fluid (liquid plus vapor) must explicitly be treated within the CRUD. This L3 milestone report summarizes the first development of these two-phase regions, accounting for resultant increases in CRUD peak temperature, determination of steaming rate, and incorporation of the capillary pressure at the liquid/vapor interface. The wick boiling assumption was eliminated in the vapor region to make this possible, resulting in a new model where the phase of the fluid in the CRUD is a coupled function of its state variables, which in turn change the homogenized material properties of each element in the CRUD simulation. Comparisons between the old and new MAMBA-BDM models are shown, with discussions on the implications for both CRUD-related issues of CILC and CRUD-induced power shift (CIPS).

2. Background

CRUD, or Chalk River Unidentified Deposits, refers to the buildup of porous corrosion deposits on the fuel rods of nuclear reactors. These heavily iron- and nickel-bearing deposits originate from the internal metallic surfaces in a light water reactor, particularly the steam generator in pressurized water reactors (PWRs), which release soluble and particulate species into the coolant. These solutes and particulates then travel via the coolant to the fuel rods, where high heat fluxes can induce sub-cooled boiling, locally drying out small patches of cladding. The solutes and particulates can then form porous deposits on the cladding surface, leading to changes in coolant flow patterns, degraded heat transfer, and accelerated corrosion (CILC) underneath the CRUD. In addition, the presence of large amount of boric acid in the coolant of PWRs, present for neutronic control, can result in the accumulation of boron compounds within the pores of the CRUD. This can lead to CIPS, where the axial power spectrum of the PWR is shifted away from these boron deposits, decreasing controllability of the reactor. Finally, the presence of so much activatable metal next to the fuel, particularly nickel and cobalt, causes the CRUD to become very radioactive, presenting health concerns to plant workers via increased radiological dose. The causes and effects of CRUD are summarized in Figure 1, along with typical photographs of CRUD in a PWR.

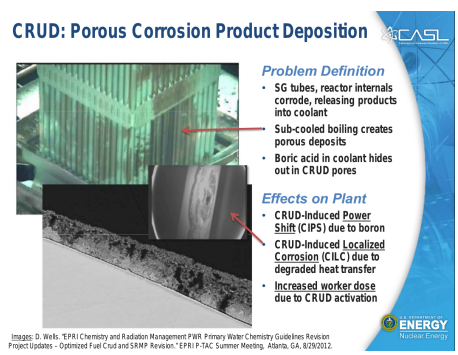

Figure 1: Summary of causes and effects of CRUD in PWRs [4]

2.1. Previous CRUD Modeling Efforts

A number of relevant existing models from the open literature will be presented next for the purposes of comparison, and to identify missing pieces that are being addressed by the MAMBA team.

2.1.1. Wick Boiling Models

The Cohen wick boiling model [6] treats the variations in temperature along a boiling chimney, inside a porous deposit with fixed porosity, pore size and tortuosity. A schematic of the model is shown in Figure 2. It is assumed that the evaporation rate of steam is determined by this temperature profile, and therefore that all evaporation takes place at the surface of the boiling chimney. This does not allow for dryout regions inside the porous deposit (CRUD). In addition, it does not alloy for 2-D variations in other parameters, such as porosity or tortuosity. Effects of this limitation will be more thoroughly described in the next subsection. Nevertheless, the simplicity of the Cohen model has led to widespread adaptation even by recent CRUD modeling efforts [5, 8], as the 1-D calculations are not CPU intensive compared to 2-D or 3-D cases.

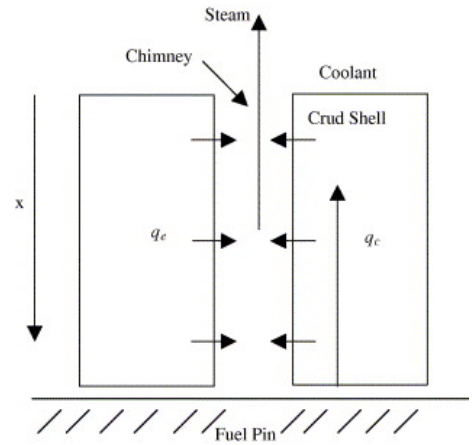

Figure 2: Schematic diagram of heat transport during wick boiling. q_e is the evaporative heat flux and q_c is the conductive heat flux. Boiling rates can vary axially along the chimney, but not radially around the chimney. [5]

The Pan wick boiling model [7] treats the CRUD around a boiling chimney in 2-D, making the equations much more involved and computationally intensive. A schematic of the outcome of this model is shown in Figure 3. The Pan model treats the concentration of an "infinitely soluble" solute (in this case, (H_3BO_3, aq)) as a result of wick boiling at the surface of the boiling chimney, accounting for changes in boiling surface and fluid transport due to porosity and tortuosity. However, the assumption of an infinitely soluble solute does not allow for realistic limits of concentration. In addition, the assumption that the boiling surface is at the boiling chimney may not be true, as limits in solute concentration would impose stricter limits on boiling point elevation compared to those in this model.

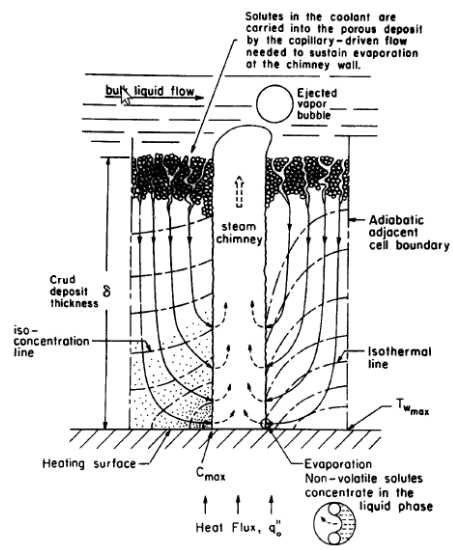

Figure 3: Schematic of the 2-D wick boiling model developed by Pan et al., showing example isothermal and isoconcentration lines around a boiling chimney in CRUD [7].

2.1.2. CRUD Chemistry Models (CCMs)

The Pan CCM (as mentioned above) treats the concentration of one infinitely soluble solute. It first analytically defines equations for any location around the boiling chimney, then solves them numerically using roughly a 50×50 mesh. The mesh is dimensionless, scaled by the size of the cell and the thickness of the CRUD. The effect of moving to a 2-D mesh instead of a 1-D analytical solution is best illustrated in Figure 4a, where the concentration of the solute is compared for the Cohen model's 1-D case, the Pan model's 1-D case and the Pan model's 2-D case. This suggests that the Cohen model would over-predict the amount of

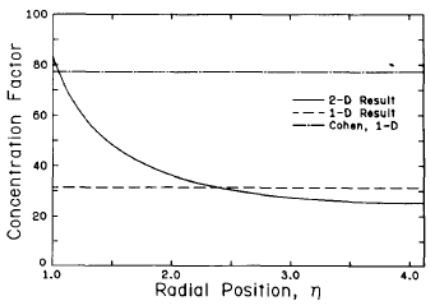

(a) Comparison of the Cohen 1-D model to the Pan 1-D and 2-D models [7]

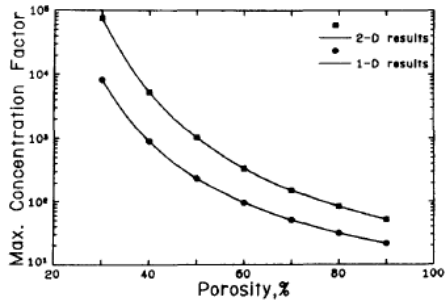

(b) Effect of varying the porosity on the maximum concentration factor in CRUD. Note that a porosity change of 20% can change the concentration by an order of magnitude [7].

Figure 4: Relevant figures from the Pan CCM

solute present, as the maximum of the 2-D case is roughly the concentration level in the 1-D Cohen model. In addition, the fact that Pan's model assumes infinite solubility will lead to further over-prediction, for dryout will limit the amount of soluble boron-bearing species that can form. In addition, the Pan model demonstrates the effect of varying the porosity on the maximum concentration factor in CRUD (see Figure 4b). Note that a porosity change of 20% can change the concentration by an order of magnitude. The model assumes a constant porosity at steady state, so allowing porosity to vary with distance and time will add a dimension of realism to the model. Finally, the Pan model takes neither radiolysis chemistry nor burning of boron in deposits into account. Nevertheless it provides an excellent starting point for a more computationally intensive model to be developed.

The Henshaw CCM [5] considers the concentration of multiple boron species coupled with a detailed chemistry model, a thermal transport model, radiolysis chemistry, depletion of boron by neutron absorption, and wick boiling. The Henshaw CCM uses the Cohen boiling model, defining it as a 1-D model. Conversations with Jim Henshaw revealed that the reason for doing so is the intended deployment of the model on an ordinary desktop computer [9]. Parameters such as thermal conductivity, CRUD porosity, pore size, CRUD tortuosity and diffusion coefficients are taken as constants, while concentrations of soluble and gaseous species can vary along the axis of the boiling chimney. In addition, Jim mentioned that good validation for using the results of the 1-D model doesn't quite exist, and it would be very useful to know how the 2-D case compares to the 1-D case [9]. This could lead to either validation or a simplified correction of existing 1-D models for easier and more accurate computation. The chemistry model is highly detailed, including forty equations for the radiolysis of water alone. These equations and their rate constants were taken from the work of Elliot et al. [10]. The results of Henshaw's model are highly significant, showing an elevated pH near the cladding wall. This in turn leads to instability of zirconia. Finally, it should be noted that the Henshaw model uses a

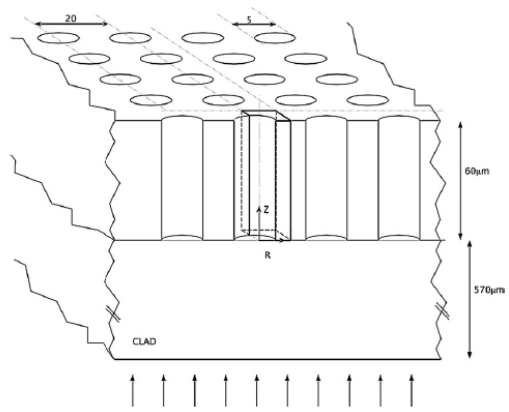

Figure 5: Schematic diagram of ul Haq's CRUD model. The model assumes this existing CRUD structure, studying changes in solute concentration and temperature distributions around a boiling chimney [8].

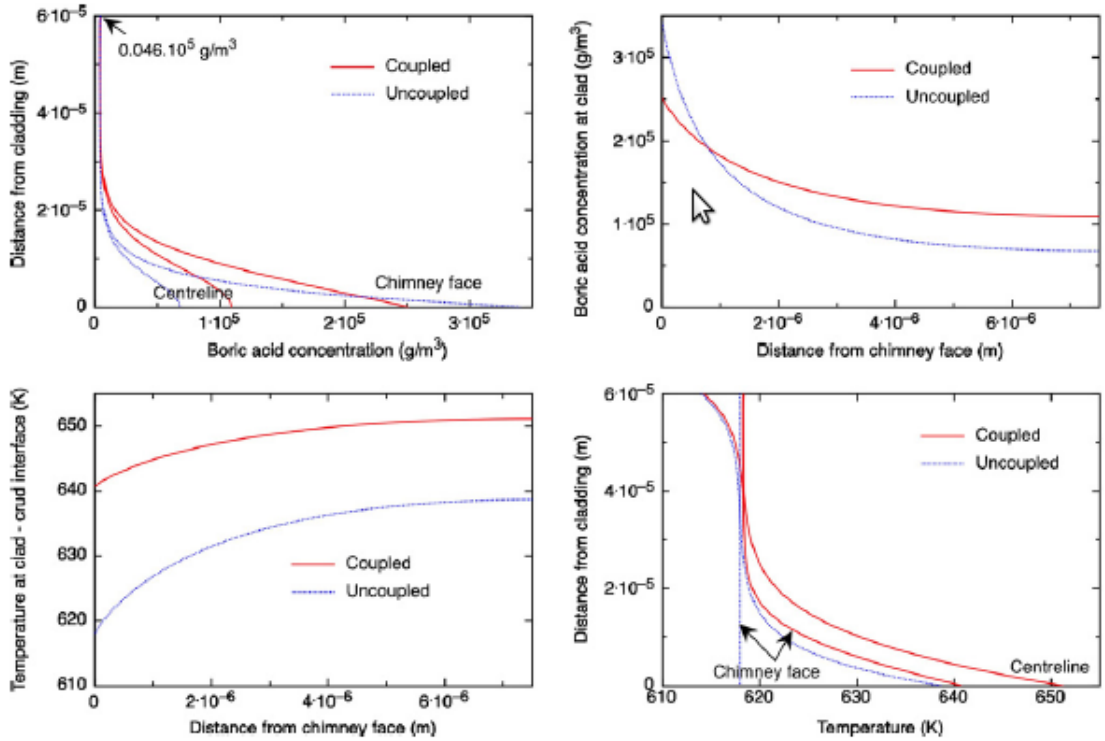

Figure 6: Results from ul Haq's model [8] compared with Pan's model [7], showing the differences in various parameters between coupled and uncoupled simulations of similar CRUD.

single chimney size and spacing.

The ul Haq CCM [8] considers a 2-D case of heat flux and solute concentration assuming existing boiling chimneys of fixed size and spacing, a schematic of which is shown in Figure 5. This CCM has a similar shortcoming to previous models (with the exception of the Henshaw model) in that it only studies the concentration of one boron-bearing species, H_3BO_3. However, it did take a large leap forward in demonstrating the difference in results for coupling the phenomena of heat transfer, solute concentration, and wicked coolant velocity. Examples of these graphs showing the difference in results between coupled and uncoupled phenomena are shown in Figure 6. This model does account for the increase in saturation temperature due to solute concentration, but again it only assumes the presence of one solute. This was done for simplicity's sake, mainly to make it easier to illustrate the effect of coupling relevant phenomena.

2.1.3. Multiphysics Models

More recently, the first results of the MAMBA-BDM multiphysics, multiscale model have been published [2]. This model incorporated fully coupled equations for homogenized CRUD temperature, liquid fluid flow, and boric acid buildup and precipitation. While many similarities existed between MAMBA-BDM and previous models, such as the assumption of wick boiling at the CRUD-chimney interface, the assumption of no heat convection by fluid was eliminated and shown to be significant in certain cases. In addition, the introduction of spatially dependent material properties coupled to the state variables in the CRUD proved useful on two counts: 1) local variations in CRUD properties and boundary conditions enabled relatively simple implementation of a full-core CIPS estimation [11], shown in Figure 7, and 2) the search for CRUD constituent material properties revealed a completely unmeasured thermal conductivity of $NiFe_2O_4$, which has

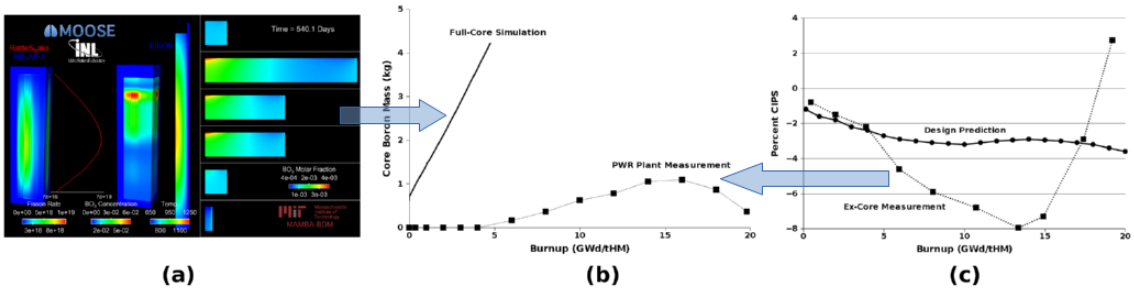

Figure 7: Example of full-core simulations using over 20,000 instances of MAMBA-BDM, with direct comparisons to plant data from EPRI [12]

since been measured in part by the MPO team [13]. Nevertheless, the older MAMBA-BDM model still required the assumption of liquid superheat temperatures of up to 12K, which is a very unphysical assumption. In addition, the low temperatures predicted by the old MAMBA-BDM at even high cladding heat fluxes were insufficient to explain the high rates of corrosion found in a number of PWRs.

2.2. Requirements for an Accurate Two-Phase CRUD Model

Before implementing an arbitrary model of two-phase flow in CRUD, a physical understanding of how boiling must occur is required. First, the decision whether to include a two-phase region (liquid and vapor mixed) must be made. Using the assumption of Darcy flow in both phases due to low flow speeds, negligible amounts of droplet entrainment in the vapor and vice versa would be expected. Next, if a region where two phases were well-mixed in steady state truly existed, in the absence of significant multiphase entrainment, the two phase region would have to be at constant temperature. However, a constant temperature region would imply a region with no potential for heat transfer, which would be physically impossible. Therefore, a separation between phases is required for this particular model.

A capillary pressure jump is generated at the interface between liquid and vapor, which is related to the surface tension of water and the spacing between CRUD particles (approximated as the average pore size):

$$P_c = \frac{2\sigma cos(\theta_c)}{\lambda_{avg}} \tag{1}$$

where σ is the surface tension of water as a function of temperature and pressure, θ_c is the contact angle of water with the CRUD (which may depend on its chemical composition), and λ_{avg} is the average pore size in the CRUD. At PWR conditions, this capillary pressure is on the order of 50 kPa.

Therefore, a series of nested simulations is required for accurate determination of both the two-phase boundary and the spatially dependent, homogenized state variables within the CRUD. First, a relatively simple heat conduction/convection simulation can be run, with homogenized material properties dependent on whether the CRUD at any location is below or above the saturation temperature for water. Correlations for CRUD thermal conductivity, fluid viscosity, permeability, etc. can be rerun to determine this phase boundary. Next, the liquid region of the CRUD can be solved using the old MAMBA-BDM model, with a small change in boundary conditions. Finally, the capillary pressure is added to the top boundary of a simulation of the vapor-only region, and then the two most important variables of peak clad temperature and steaming rate can be obtained. Figure 8 shows a schematic of how this simulation should be run.

Subsequent iterations, using the results of one iteration as the initial conditions for the next, can be applied while changing boundary condition assumptions to converge towards a steady solution.

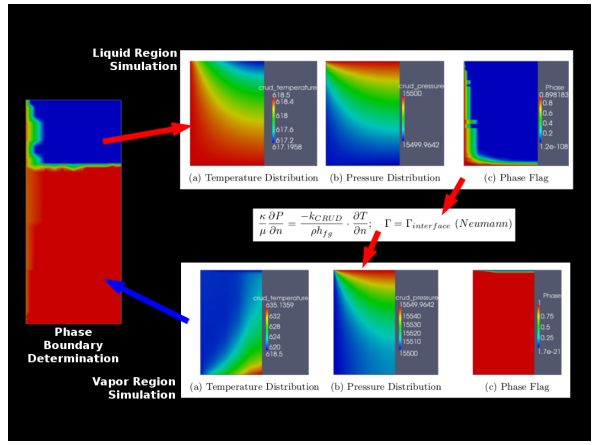

Figure 8: Schematic of how two phase MAMBA-BDM simulations are ideally run (manually now, automatically soon)

3. Changes to MAMBA-BDM's Framework

For brevity's sake, only the changes implemented in the new two-phase MAMBA-BDM model will be presented here. Anything not presented may be assumed to be identical to the MAMBA-BDM model as recently published in *J. Nucl. Mater.* [2].

3.1. Overall Description

3.1.1. Fluid Phase Variable

A new variable to track the phase was first added to MAMBA-BDM, which simply gives a value of zero for liquid and one for vapor. This phase variable is a simple, smoothed function of the homogenized CRUD temperature at any given point. Rather than choose a sharp cutoff function, some small degree of smoothing was artificially introduced to avoid discontinuities in material properties throughout the CRUD. Initial simulations with a sharp phase variable failed to converge, while a small degree of smoothing (spanning no more than 1-2 elements) achieved far faster convergence. This is simply a numerical technique to achieve simulation convergence, hopefully without noticeably affecting the final solution. Future studies will determine the influence of this phase variable width on key postprocessed solution results, such as peak clad temperature.

3.1.2. Liquid Region Boundary Conditions

The region of the CRUD facing the coolant will be at a lower temperature, as it is farther from the cladding heat source and closer to the sub-cooled bulk coolant. Therefore, constituent equations and boundary conditions in the liquid region are similar to those in the old MAMBA-BDM, including wick boiling at the chimney, with the exception of the liquid/vapor interface. Here, boundary conditions are taken to be exactly the same as at the CRUD-chimney interface, as wick boiling should now occur *both* at the boiling chimney and within the CRUD itself. These boundary equations take the following forms:

$$T = T_{sat}\left(P, C_i\right) \qquad \Gamma = \Gamma_{l/v} \tag{2}$$

$$\frac{\kappa}{\mu}\frac{\partial P}{\partial \overrightarrow{n}} = \frac{-k_{CRUD}}{\rho h_{fg}} \cdot \frac{\partial T}{\partial \overrightarrow{n}} \qquad \Gamma = \Gamma_{l/v} \tag{3}$$

where T is the homogenized CRUD temperature at the boundary, T_{sat} is the saturation temperature of water at the pressure and with chemical species concentrations present in the CRUD, Γ refers to a system boundary, $\Gamma_{l/v}$ is the liquid/vapor region boundary as found in the initial simulation for phase boundary determination, κ is the permeability of the CRUD to liquid, μ is the viscosity of liquid in the CRUD, P is the pressure in the CRUD, k is the homogenized thermal conductivity of the CRUD, ρ is the density of the liquid in the CRUD, and h_{fg} is the enthalpy of vaporization of water.

3.1.3. Vapor Region Boundary Conditions

Within the vapor region, the fundamental symbolic equations for CRUD heat transfer and fluid flow are almost identical to the liquid region, with the exception of substituting correlations for water vapor properties in the homogenized CRUD material properties instead of liquid ones. However, the boundary conditions of the vapor region must change to achieve closure. First, the capillary pressure due to the two-phase boundary must be added to the liquid/vapor boundary in the CRUD:

$$\frac{\kappa}{\mu}\frac{\partial P}{\partial \overrightarrow{n}} = \frac{-k_{CRUD}}{\rho h_{fg}} \cdot \frac{\partial T}{\partial \overrightarrow{n}};\ P_v(\Gamma) = P_l(\Gamma) + P_c \qquad \Gamma = \Gamma_{l/v} \tag{4}$$

where P_c is the capillary pressure as defined in Equation 1. In addition, the pressure of the vapor in the boiling chimney must decrease as one travels up the boiling chimney. Therefore, either a simple linear function $\mathrm{P} = \mathrm{P}(\mathrm{z})$ or a standard friction pressure loss term:

$$P(z) = P_{coolant} + P_c + f\frac{z}{D_h}\frac{\rho v(z)^2}{2} \tag{5}$$

where$P_{coolant}$ and P_c are the coolant and capillary pressure terms respectively, f is the friction factor in the chimney, assumed to be $\frac{64}{\mathrm{Re}}$ where Re is the Reynolds number for vapor flow, L is the chimney height, also known as the CRUD thickness, D_h is the chimney diameter, and $v(z)$ is the axially dependent velocity of the vapor in the chimney. The only undetermined quantity is the axial velocity distribution of vapor in the boiling chimney, which also determines the Reynolds number. This can be assumed to be linear, since one can approximate the mass flow rate of vapor into the chimney from any height z as constant, and since the mass flow rate $(\dot{\mathrm{m}})$ is given by:

$$\dot{m} = \rho v A_c \tag{6}$$

and the vapor has roughly constant density with a constant chimney cross sectional area, then $\dot{m}$ and v are linearly proportional.

3.2. Correlations and Boundary Conditions Changed in MAMBA-BDM

In addition to incorporating the new thermal conductivity model for $NiFe_2O_4$, correlations for viscosity, density, thermal conductivity, and specific heat capacity of water vapor were added to MAMBA-BDM. In addition, contact angles and surface tension correlations of liquid water at saturation were added, in order to compute the capillary pressure.

4. New Results

4.1. Two-Phase Modeling Results

For the following results, Table 1 summarizes the fixed conditions chosen for this particular CRUD simulation. Note that no boric acid or soluble lithium was included in this study, effectively turning off the chemistry modules.

Parameter	Value	Units
CRUD Thickness	25	μm
Width of CRUD Around Chimney	10.5	μm
λ_{avg} (average pore size)	0.375	μm
Coolant Temperature	600	K
System Pressure	15.5	MPa
Boric Acid Concentration	0	ppm
CRUD Porosity	50	%
Cladding Heat Flux	1	$\frac{\mathrm{MW}}{\mathrm{m}^2}$
Heat Transfer Coefficient at Coolant	12,000	$\frac{\mathrm{W}}{\mathrm{m}^2\mathrm{K}}$

Table 1: Simulation parameters chosen for the CRUD cases in this study

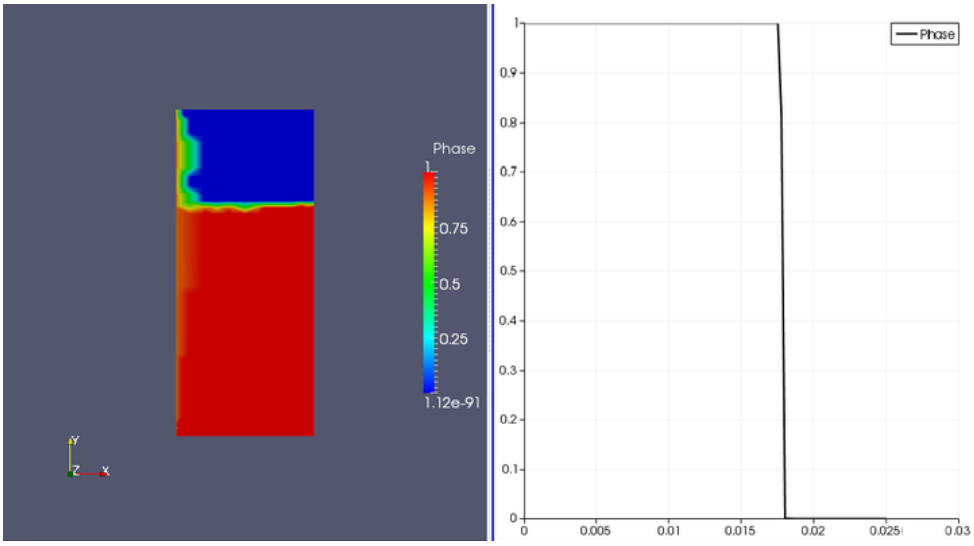

Figure 9: Simulation result and line plot through the center of the CRUD of the phase variable, showing sharp, yet smooth, variation imposed between phases

This was done to treat the effects of flow and precipitation separately, these will be addressed together in a later simulation.

First, an initial simulation without capillary pressure was performed to determine the estimated location of the two-phase boundary. These results are summarized in Figure 9. Using these results, the vapor phase region in this simulation ranged from the cladding surface to approximately 18 microns up the CRUD. Separate liquid and vapor simulations were performed using the boundary conditions and material properties as described in Sections 3.1.2-3.1.3, these results are shown in Figure 10.

4.2. Comparison of One-Phase and Two-Phase Results

A comparison of the old MAMBA-BDM code run under identical imposed conditions with the new code is shown in Figure 11. The difference is clear, the two phase model predicts a peak clad temperature of 645.6K, while the old model predicts a peak clad temperature of 630.0K. In particular, one can easily see a higher density of contour lines in the vapor region of the two phase simulation compared to the sparser lines in the single phase simulation, indicating a steeper temperature gradient. This is principally due to a very small thermal conductivity of water vapor compared to liquid water, which each make up 50% of the homogenized volume of CRUD in their respective parts of each simulation.

5. Discussion

The results above demonstrate the capabilities to perform two-phase simulations on the mesoscale level, to determine CRUD conditions at very localized spots. This is most useful for more accurate determination of CILC risk, using the same methodology in the full-core, MAMBA-BDM informed simulations performed earlier this year [11]. In one recent HOGNOSE simulation, it was shown that a temperature increase from 600K to 633K made the difference between remaining in asymptotic (slow) corrosion and breakaway (fast) corrosion in one fuel cycle (see Figure 12). The 15K temperature difference in the results above, for the case of Arrhenius limited corrosion, would result in a 100% increase in corrosion rate. However, compounded with the phase change and oxide fracture observed in Zircaloy, this 15K difference can shift

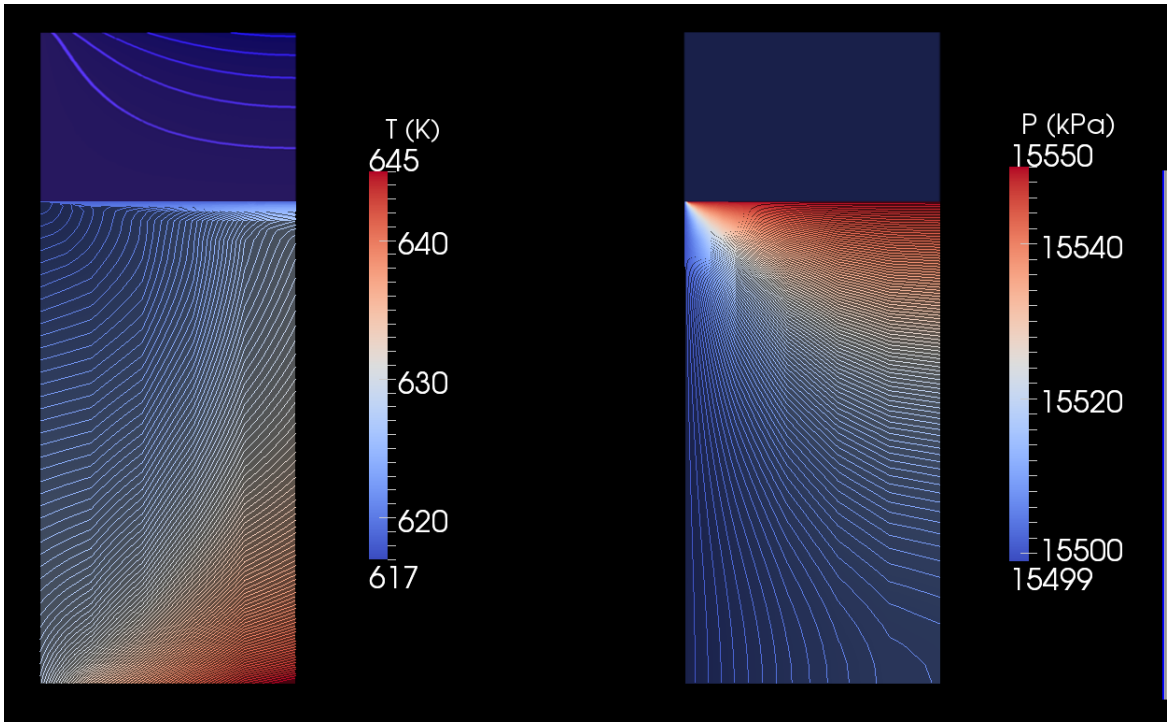

Figure 10: Two-phase simulation results, showing large temperature and pressure changes in the vapor region. Contour lines of 0.25K are drawn for convenience.

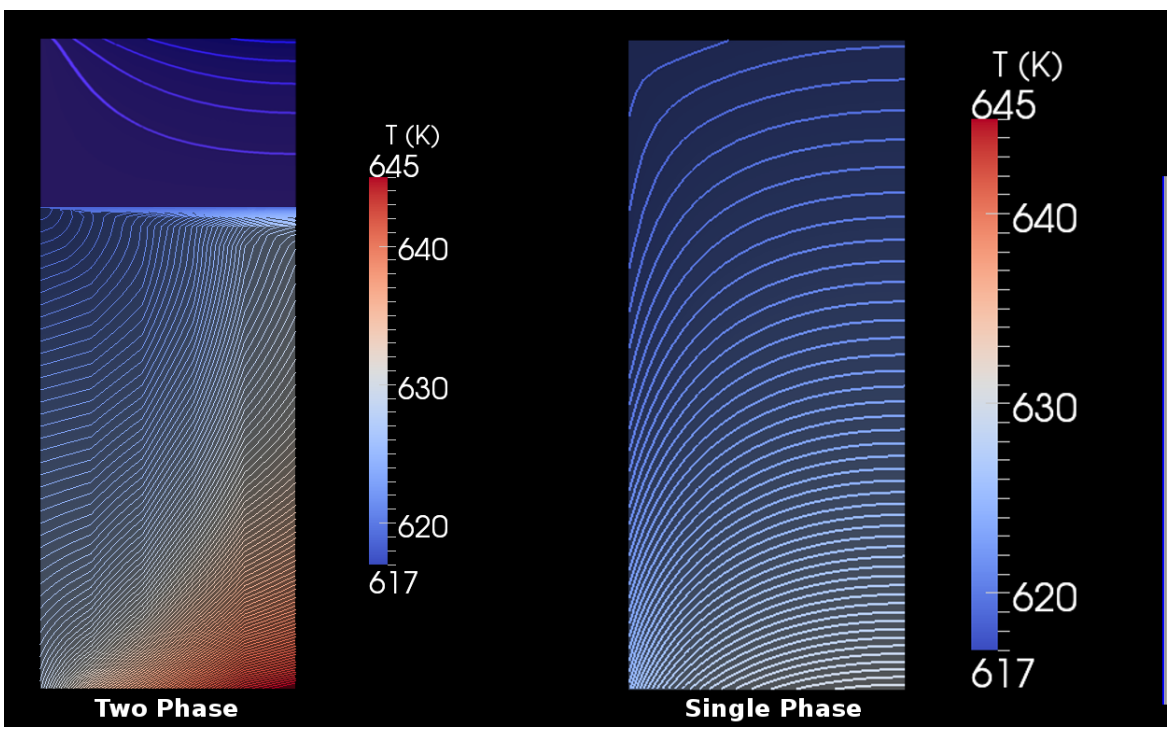

Figure 11: Comparison of two phase and single phase simulation results, showing differences in CRUD temperature distribution. Contour lines of 0.25K are drawn for convenience.

the transition to breakaway oxidation much sooner in the fuel cycle. This sudden, temperature-dependent transition underscores the importance of a two-phase model in MAMBA-BDM, and merits a new full-core CILC risk investigation with this newly recognized temperature increase.

Of course, the results shown here are for a single set of conditions. Following some short work to automate the discovery of the phase boundary location, many scripted instances of the new code will be used to plot peak cladding temperature, maximum possible CIPS risk, and steaming rate as functions of parameters like coolant temperature, cladding heat flux, CRUD porosity, CRUD composition, and CRUD thickness. In particular, it is expected that the vapor dryout region of CRUD will form rather quickly for existing CRUD, while the CRUD itself will grow quite slowly. This slow change in CRUD thickness will be coupled directly to the size of the liquid/vapor regions via the steaming rate, or the rate of liquid evaporation, since the solutes that enter with fresh coolant get deposited as the steam leaves the CRUD. The CRUD growth rate at any given time could be approximated as follows:

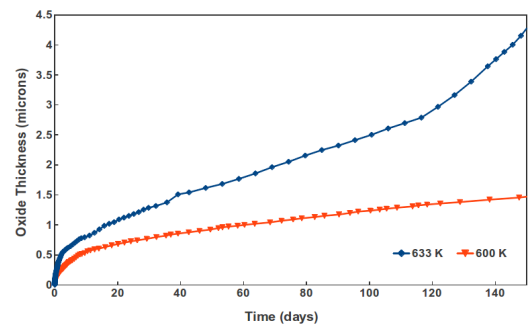

Figure 12: HOGNOSE simulation showing transition to breakaway corrosion by increasing temperature [3]

$$\frac{\partial t_{CRUD}}{\partial t} \propto dt \cdot \left[\dot{m}_{steaming} \cdot \left[\sum_{i=1}^{n} \left[K_i \cdot C_{i,soluble} + \dot{m}_{i,particulate} \right] \right] - K_2 \cdot TKE \right] \tag{7}$$

where dt is the length of a timestep (may be variable) in a simulation, $\dot{m}_{steaming}$ is the rate of evaporation of coolant around one chimney, K_i is a factor describing a precipitation rate, $C_{i,soluble}$ is the concentration of a soluble species in the CRUD, *TKE* is turbulent kinetic energy (a measure of fluid erosion on the CRUD surface), and K_2 is a proportionality constant relating *TKE* to erosion rate. In this way, postprocessed values of $\dot{m}_{steaming}$ can lead to a particular CRUD growth rate at any given time along with known, external reactor coolant parameters (coolant soluble & particulate concentrations and TKE). In this way, the full core simulations from [11] can determine their own CRUD growth rates, rather than using prescribed

6. Future Work

6.1. Areas for Improvement

While two-phase flow simulation has now been demonstrated to be physically significant, much work remains in refining the models, in particular the choices of boundary conditions, as well as linking this mesoscale model to a full-core simulation. Areas of future work are summarized below.

6.1.1. Short Term

1. Automation of the two-phase simulation process (to avoid three separate, hand-coded simulations) using the MOOSE MultiApp and Transfer system
2. Return of the MAMBA-BDM chemistry models, with re-estimation of CIPS risk as a result of the vapor dryout region

3. Direct incorporation of CRUD growth using the mesh displacement feature available in MOOSE through LibMesh
4. The inclusion of chemical reaction kinetics for the formation, precipitation and dissolution of other Li- and B-bearing species than boric acid (and resultant metaborite or boron oxide)
5. The inclusion of an added zirconia source term to the CRUD from debris created by GTRF [14]
6. Verification of MAMBA-BDM's real CRUD modeling capability with plant measurements of CRUD and CILC from recent EPRI reports

6.1.2. Long Term

1. Verification of behavior during a reactor transient, a trip, or a shutdown with observed plant AOA results
2. Verification of CIPS behavior modeled by MAMBA-BDM with that measured in operating PWRs (demonstrated for the KAIST-3A core, desired to repeat for the AP-1000)
3. Exploration of the risk of CILC based on CRUD parameters, such as maximum clad temperature, pH and lithium concentration adjacent to the clad
4. Informing the code with 3D information by using CFD and DNS studies, to account for circumferential variations in CRUD parameters around a boiling chimney without needing to perform a full 3D simulation
5. Generation of lookup tables as functions of many variables and operating history, to speed up calculation of macroscale CRUD properties by the MAMBA-BDM CRUD growth program (which calls this boron deposition model)

7. Acknowledgements

The authors wish to acknowledge many helpful discussions with Prof. Jacopo Buongiorno (MIT), as well as discussions with Brian Kendrick and Chris Stanek (both of LANL), and all the attendees of the MPO/P-TAC meetings over the past year.

[1] M. P. Short and et al. Linking length scales, simulations, and experiments in the study of PWR Fuel CRUD and CRUD-induced localized corrosion (CILC). In *Multiscale Materials Modeling*, Biopolis, Singapore, October 2014. MRS-Singapore.

[2] M. P. Short, T. Besmann, D. Hussey, B. K. Kendrick, C. Stanek, D. Gaston, J. Li, C. Permann, and S. Yip. Multiphysics modeling of porous crud deposits in nuclear reactors. *J. Nucl. Mater.*, 443(1-3):579–587, 2013.

[3] A. Dykhuis, M. Youseff, B. Yildiz, and M. P. Short. L4 milestone report: Oxide phase transition incorporation into hognose zircaloy corrosion model. Technical report, CASL-MPO, December 2013.

[4] M. P. Short et al. Finding the cure to crud. In *Meeting between MIT and CRIEPI*, Yokosuka, Japan, November 3 2013. Central Research Institute for Electric Power Industry (CRIEPI).

[5] J. Henshaw, J. C. McGurk, H. E. Sims, A. Tuson, S. Dickinson, and J. Deshon. A model of chemistry and thermal hydraulics in PWR fuel crud deposits. *J. Nucl. Mater.*, 353(1-2):1–11, July 2006.

[6] P. Cohen. Heat and mass transfer for boiling in porous deposits with chimneys. *AlChE Symp. Ser.*, 70:71, 1974.

[7] C. Pan, B. G. Jones, and A. J. Machiels. Concentration levels of solutes in porous deposits with chimneys under wick boiling conditions. *Nucl. Eng. Des.*, 99:317–327, February 1987.

[8] I. Haq, N. Cinosi, M. Bluck, G. Hewitt, and S. Walker. Modelling heat transfer and dissolved species concentrations within PWR CRUD. *Nucl. Eng. Des.*, 241(1):155–162, January 2011.

[9] M. P. Short and J. Henshaw. Conversations between Short and Henshaw at the 2010 EPRI P-TAC meeting. February 2010.

[10] A. J. Elliot, D. R. McCracken, G. V. Buxton, and N. D. Wood. *J. Chem. Soc. Faraday Trans.*, 86:1539, 1990.

[11] D. R. Gaston et al. Physics-based multiscale coupling for full core nuclear reactor simulation. *Annals of Nuclear Energy*, (submitted), 2014.

[12] M. P. Short, D. R. Gaston, C. R. Stanek, and S. Yip. A perspective on coupled multiscale simulation and validation in nuclear materials. *MRS-B*, 39:71–77, 2014.

[13] A. T. Nelson et al. Thermal expansion, heat capacity and thermal conductivity of nickel ferrite (NiFe2O4). Tech. Report Number LA-UR-13-28786, Los Alamos National Laboratory, 2013.

[14] M. P. Short, I. Bolotnov, and M. J. Demkowicz. Assessment of cfd/crud/gtrf coupling strategies for vera integration. Casl/mpo l4 milestone report, CASL/MPO - MIT, NCSU, November 2011.